PHYSICAL REVIEW B VOLUME 27, NUMBER 6 15 MARCH 1983

# Electronic properties of bulk copper-aluminum and copper-zinc alloys

K. R. Mountfield and J. A. Rayne
*Department of Physics, Carnegie-Mellon University, Pittsburgh, Pennsylvania 15213*

(Received 2 August 1982)

Magnetic-susceptibility, as well as resistivity, Hall-effect, transverse-magnetoresistance, and thermoelectric-power, measurements have been made on a series of well-characterized bulk samples covering the entire copper-aluminum and copper-zinc phase diagrams. In both systems the resistivity of the $\gamma$ phase exhibits a sharp minimum as a function of composition. This minimum correlates with anomalies observed in the other measured properties and supports the hypothesis that the behavior is due to electronic effects associated with overlap between the Fermi surface and the Jones zone for this structure. Comparison of the properties of other phases in the two systems indicates similarities which can be also ascribed to band-structure effects.

## I. INTRODUCTION

The copper-aluminum system, which is of considerable importance in integrated circuit technology, is also of intrinsic physical interest. Recent measurements on bulk alloys[1] have shown that the resistivity of the $\gamma_2$ phase exhibits a very strong dependence on composition. This behavior has been ascribed to electronic effects associated with contact between the Fermi surface and the Jones zone for the structure. Electronic effects are also observed in the conduction properties of other phases, in particular the values of $d\rho/dc$ for the primary solid solutions *Cu*Al and *Al*Cu.

Hitherto there has been no systematic study of the transport and magnetic properties of bulk copper-aluminum alloys to investigate in detail the influence of electronic structure. The present work reports measurements of the magnetic susceptibility, as well as Hall effect, transverse magnetoresistance and thermoelectric power, on well-characterized bulk samples covering the entire phase diagram of this system. Data are also presented for bulk samples spanning the phase diagram of the copper-zinc system, including extensive measurements on the $\gamma$-phase alloys which have a structure similar to that of the $\gamma_2$ phase of copper-aluminum. The results show conclusively that overlap effects between the Fermi zone and Jones surface are dominant in each of the latter phases, but that interesting differences are observed in their detailed behavior. Comparison of the properties of other phases in the two systems indicate similarities which can also be ascribed to band-structure effects.

## II. EXPERIMENT

Reference to Table I shows that, in addition to the cubic primary solid solutions, there are five intermediate phases in the copper-aluminum system. Both $\gamma_2$ and $\delta$ are complex cubic structures, the former having the approximate composition $Cu_9Al_4$ with a stability range extending from 31 to 37 at. %. There is some disagreement about the structure of the $\delta$ phase,[2] which occurs near 40 at. % aluminum corresponding to the composition $Cu_3Al_2$. The remaining phases $\zeta_2$, $\eta_2$, and $\theta$ are electron compounds with approximate formulas $Cu_4Al_3$, CuAl, and $CuAl_2$, respectively. The structure of the $\zeta_2$ phase is also in doubt.

Table I also shows the well-known phases of the copper-zinc system. Here the zinc-rich primary solid solution is the hexagonal $\eta$ phase, in contrast to the cubic $\alpha$ phase, which is of the classic Hume-Rothery type. The $\gamma$ phase, with the approximate composition $Cu_5Zn_8$, is similar in structure to the $\gamma_2$ phase of the copper-aluminum system. Neither the familiar cubic $\beta'$ phase, which undergoes an order-disorder transformation to $\beta$ at 456° C, nor the hexagonal $\epsilon$ phase with the nominal formula $CuZn_5$ requires further comment.

Samples of alloys covering both the copper-zinc and copper-aluminum systems were prepared by induction melting 99.999%-pure constituents under an argon atmosphere. The copper-aluminum ingots were prepared in recrystallized alumina crucibles, while the copper-zinc ingots were melted in high-purity carbon crucibles. The latter were fitted with tightly fitting, tapered lids to prevent loss of zinc

TABLE I. Properties of phases in copper-aluminum and copper-zinc systems. (See Ref. 2).

| System | Phase | Nominal composition | Lattice | Space group |
|---|---|---|---|---|
| Cu-Al | $\alpha$ | (Cu) | Cubic | *Fm* 3*m* |
| | $\gamma_2$ | $Cu_9Al_4$ | Cubic | $P\bar{4}3m$ |
| | $\delta$ | $Cu_3Al_2$ | Cubic | $I\bar{4}3m$ |
| | $\zeta_2$ | $Cu_4Al_3$ | Monoclinic | |
| | $\eta$ | CuAl | Monoclinic | $C2/m$ |
| | $\theta$ | $CuAl_2$ | Tetragonal | $I4/mcm$ |
| | $\beta$ | (Al) | Cubic | *Fm* 3*m* |
| Cu-Zn | $\alpha$ | (Cu) | Cubic | *Fm* 3*m* |
| | $\beta(\beta')$ | CuZn | Cubic | *Im* 3*m* (*Pm* 3*m*) |
| | $\gamma$ | $Cu_5Zn_8$ | Cubic | $I\bar{4}3m$ |
| | $\epsilon$ | $CuZn_5$ | Hexagonal | $P6_3mc$ |
| | $\eta$ | (Zn) | Hexagonal | $P6_3mc$ |

during the melting process. After casting the ingots were annealed for several days in argon, close to the maximum temperature consistent with stability, as determined from the relevant part of the phase diagram. They were then water quenched from annealing temperature to prevent solute precipitation. X-ray data taken on powder samples prepared from the quenched ingots gave lattice parameters in good agreement with accepted values.[2] The alloy compositions were determined from the starting masses of the constituent metals. Differences between the latter and the mass of the resulting ingot were in all cases less than 20 mg, corresponding to an uncertainty in composition of less than 0.1 at. %.

All the samples used in this work were spark cut from adjacent positions in the same ingot. The resistivity specimens were in the form of rectangular parallelopipeds approximately 2 cm long and of $1.5\times1.5$ mm cross section. Measurements of resistance and transverse magnetoresistance were made by the usual four-probe method using an automated apparatus, details of which have been published in a previous paper.[3] The magnetoresistance measurements were made up to fields of 23 kG, using a 12-in. Varian electromagnet with tapered iron-cobalt pole caps. Susceptibility data were obtained, with a standard Faraday balance using constant-gradient pole caps, on sections of the same specimens used for the resistance measurements.

In order to obtain sufficient sensitivity for the Hall measurements, separate samples approximately 0.2 mm thick and 3 mm in width were spark cut from the ingots. As will become evident later, the large grain size in some of the copper-zinc ingots caused problems in obtaining Hall data for the hexagonal phases. Data were obtained up to 23 kG, with same magnet used for the magnetoresistance experiments.

Thermoelectric measurements were made on the Hall samples, using a standard technique in which the thermoelectric emf $V$ of a copper-alloy couple is measured as a function of the temperature difference across the couple. The resulting value of thermoelectric power of the alloy relative to copper was then obtained from the relation $\Delta S = S_{\text{alloy}} - S_{\text{Cu}} = dV/dT$. From the known value of $S_{\text{Cu}}$ the thermoelectric power of the alloy could then be computed.

## III. RESULTS

The variation of resistivity as a function of composition for the copper-aluminum and copper-zinc systems is shown in Figs. 1 and 2, respectively. At low solute concentrations the usual linear dependence is observed, the values of $d\rho/dc$ being in good

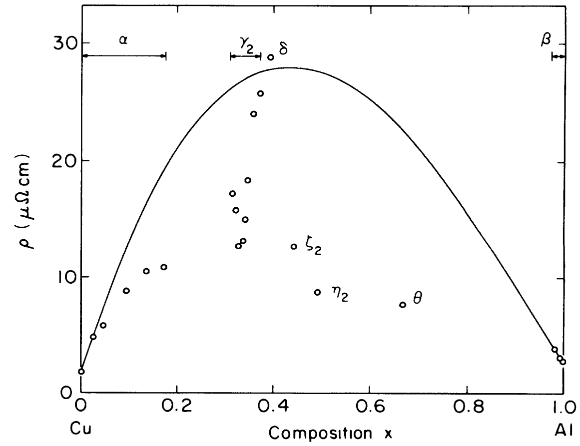

FIG. 1. Variation of resistivity at 295 K as a function of composition $x$ in $Cu_{1-x}Al_x$ alloys. Solid curve is the concentration dependence predicted by virtual-crystal model discussed in text.

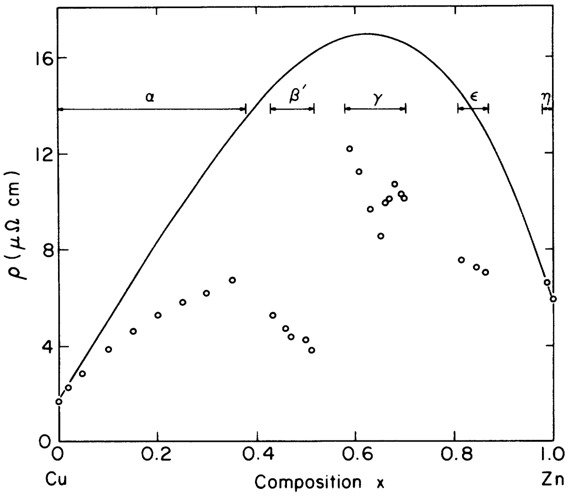

FIG. 2. Variation of resistivity at 295 K as a function of composition $x$ in $Cu_{1-x}Zn_x$ alloys. Solid curve is the concentration dependence predicted by virtual-crystal model discussed in text.

agreement with previous determinations[4,5] except in the case of *Zn*Cu where independent data are not available. For higher concentrations in *Cu*Al and *Cu*Zn nonlinearity due to solute interaction effects is observed.

The most salient feature of the results for the intermediate phases of the copper-aluminum system is the very high resistivity of the $\gamma_2$ and $\delta$ phases and the pronounced minimum in the former as a function of composition. This behavior also occurs in $\gamma$-CuZn, although the magnitude of the minimum is somewhat smaller in this case. Previous measurements[6,7] on the latter phase have yielded contradictory results, one set of data showing an essentially continuous variation with composition and the other a complex oscillatory dependence. No reason can be advanced for the disagreement with the present work. The resistivities of the $\zeta_2$, $\eta_2$, and $\theta$ phases in the copper-aluminum system, as well as the ordered $\beta'$ phase and $\epsilon$ phase in copper-zinc, are similar to those observed in polyvalent pure metals.

Figures 3 and 4 show the composition dependence of the magnetic susceptibilities for copper-aluminum and copper-zinc. For both the primary solid solutions *Cu*Al and *Cu*Zn the diamagnetic susceptibility increases slowly with increasing solute concentration, the observed changes again being in good agreement with previous measurements.[8-10] For *Al*Cu and *Zn*Cu alloying also produces a diamagnetic change in the susceptibility, although in the former case there is a net paramagnetism in the alloy due to the magnetic properties of the dominant aluminum ions. No susceptibility data have been previously reported for these phases.

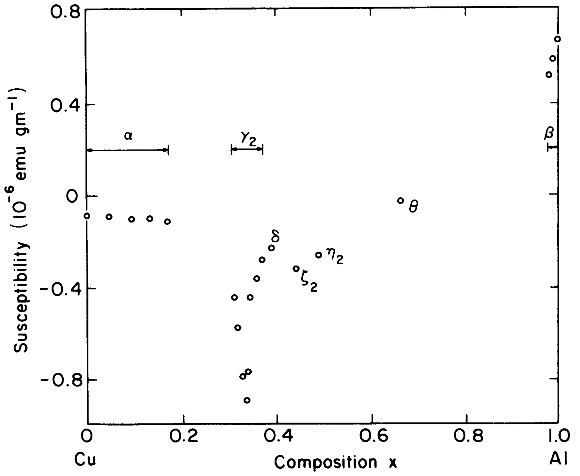

FIG. 3. Variation of susceptibility at 295 K as a function of composition $x$ in $Cu_{1-x}Al_x$ alloys.

As can be seen from Figs. 3 and 4 both the $\gamma$ phase in copper-zinc, as well as the $\gamma_2$ and $\delta$ phases in copper-aluminum, show very large peaks in the diamagnetic susceptibility as a function of composition. Previous measurements on $\gamma$-phase alloys of the copper-zinc type[7,8,10,11] have shown similar behavior. The present data, taken on identical specimens, show that the compositions corresponding to the minima in resistivity are not the same as those corresponding to the maxima in diamagnetic susceptibility. In particular, the former occur at 32.5 at. % aluminum and 65.2 at. % zinc, while the latter occur at 33.3 at. % aluminum and 66.9 at. % zinc, respectively. Essentially identical behavior is observed at 77 and 4.2 K. The magnetic properties of the remaining phases in both systems are not unusu-

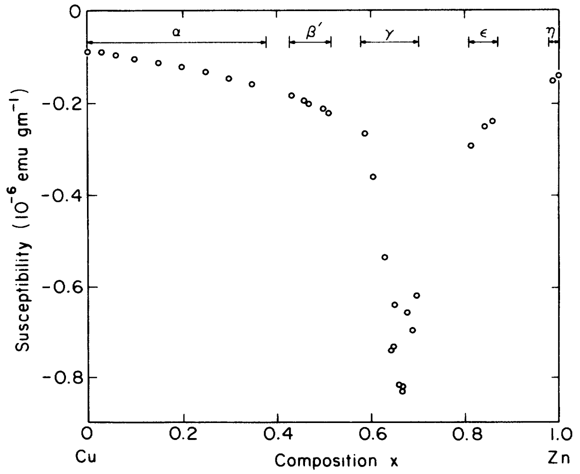

FIG. 4. Variation of susceptibility at 295 K as a function of composition $x$ in $Cu_{1-x}Zn_x$ alloys.

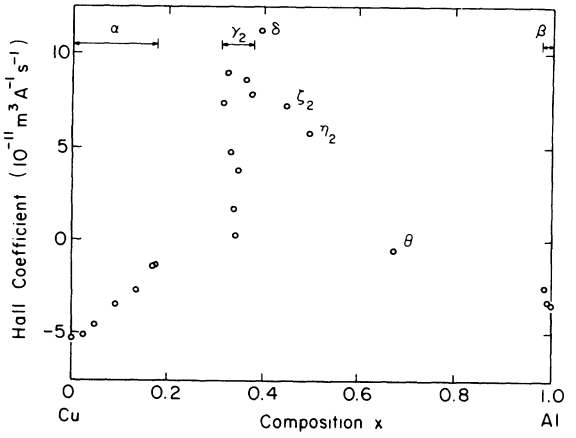

FIG. 5. Variation of Hall coefficient at 295 K as a function of composition $x$ in $Cu_{1-x}Al_x$ alloys.

al. It is of interest that the $\theta$ phase of copper-aluminum has essentially no magnetic susceptibility, while the $\zeta_2$ and $\eta_2$ phases are strongly diamagnetic.

Figures 5 and 6 show that the behavior of the Hall coefficient of the primary solid solutions *Cu*Al, *Cu*Zn, and *Al*Cu corresponds to predominantly electron carriers. The composition dependence obtained for the first two phases is in good agreement with earlier work[12]; no previous data have been reported for *Al*Cu. As can be seen from Fig. 6, the coefficients for the hexagonal $\epsilon$ and $\eta$ phases in the copper-zinc system show significant variation, depending on the position of the voltage probes along the sample. This behavior simply results from the large grain size in the samples and the fact that in hexagonal crystals the Hall coefficient is anisotropic. Comparison of the present results with single crystal data[13] for the $\eta$ phase of the copper-zinc system indicate that there is a preferred orientation in our samples, corresponding to the magnetic field being normal to the $c$ axis.

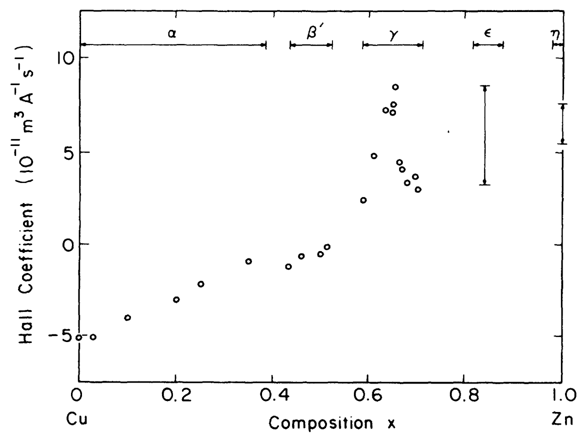

FIG. 6. Variation of Hall coefficient at 295 K as a function of composition $x$ in $Cu_{1-x}Zn_x$ alloys. Arrows indicate the range of values associated with anisotropy of $R$ discussed in text.

Both the $\gamma_2$ and $\delta$ phases of copper-aluminum and the $\gamma$ phase of copper-zinc have positive Hall coefficients, corresponding to predominantly hole conduction. It can be seen that the composition dependence is quite different in the two cases. For copper-zinc the Hall coefficient shows a sharp maximum at 65.2 at. % zinc, while in copper-aluminum there is a sharp minimum at 33.7 at. % aluminum. In the latter system there are subsidiary maxima near the terminal compositions for the $\gamma_2$ phase. The present data for $\gamma$-CuZn agree reasonably well with those previously reported by Hishiyama[6] but differ significantly from those of Menth,[7] who found an oscillatory dependence on composition. No reason for the latter discrepancy can be advanced, other than to ascribe it to differences in the metallurgy of the specimens used in the two experiments. In the case of $\gamma_2$-CuAl, the behavior found here differs somewhat from that found by Hishiyama for lower electron concentrations. This disagreement is not understood.

The $\zeta_2$ and $\eta_2$ phases of copper-aluminum, for which data have not previously been reported, both have positive Hall coefficients corresponding to hole conduction. This behavior is to be contrasted to that of the $\theta$ phase, which has a very small negative coefficient indicative of an overall net electronic conductivity. The ordered $\beta'$ phase of copper-zinc also behaves in the same way, in agreement with previous measurements.[14]

In the primary solid solutions for both systems, the magnetoresistance changes $\Delta\rho/\rho$ are too small to be accurately measured with the fields conveniently available. The largest effects are observed in the $\gamma$-phase alloys, which exhibit resistance changes several orders of magnitude higher than those observed in pure metals at room temperature. As expected, the magnetoresistance obeys a quadratic field dependence up to the maximum available field (23 kG). Figure 7 shows the composition dependence of the coefficient $A$, in the relation $\Delta\rho/\rho = AH^2$, for both systems. It is clear that in each case $A$ rises to a maximum value at essentially the same composition as that corresponding to the minimum in resistivity. For $\gamma$-CuZn there is evidence of structure at higher zinc concentrations, paralleling that observed in $\rho$. The magnetoresistance in $\delta$-CuAl is quite small, again showing that it is very similar in its properties to the $\gamma_2$ phase. From Fig. 7 it can be seen that the $\zeta_2$, $\eta_2$, and $\theta$ phases in copper-aluminum also have low values of $A$.

Reference to Figs. 8 and 9 shows that the thermoelectric power for the primary solid solutions

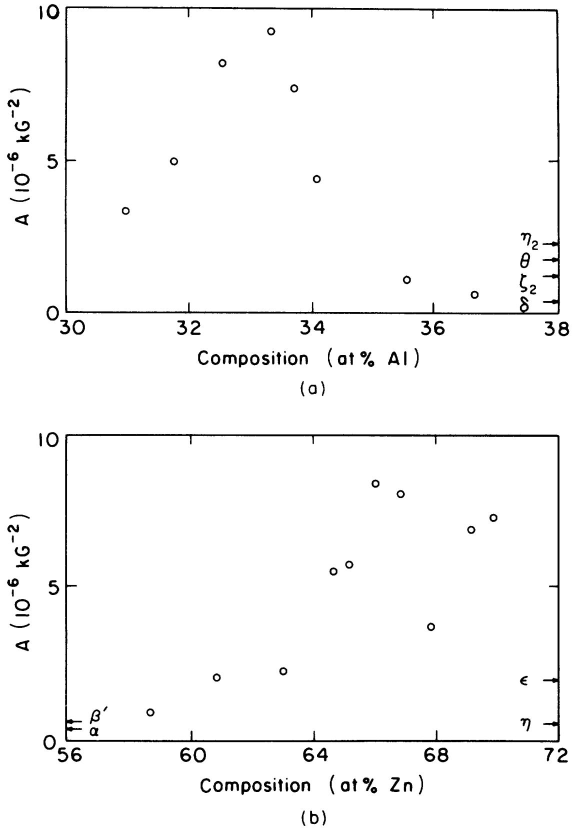

FIG. 7. Variation of magnetoresistance coefficient $A=(1/H^2)\Delta\rho/\rho$ as a function of composition in (a) copper-aluminum and (b) copper-zinc $\gamma$-phase alloys. Arrows indicate values of $A$ for remaining phases in each system. Note that coefficients for terminal solid solutions in copper-aluminum are negligibly small on this scale.

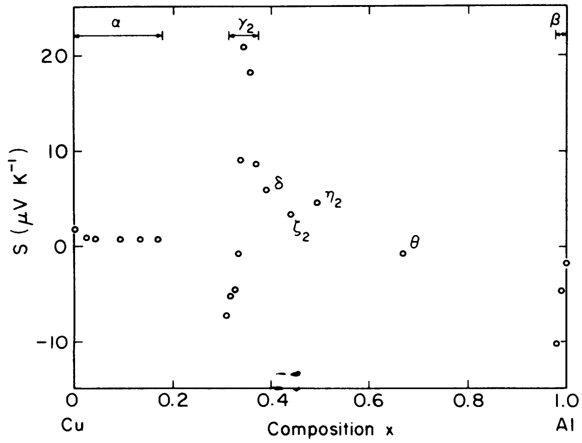

FIG. 8. Variation of thermoelectric power at 295 K as a function of composition $x$ in $Cu_{1-x}Al_x$ alloys.

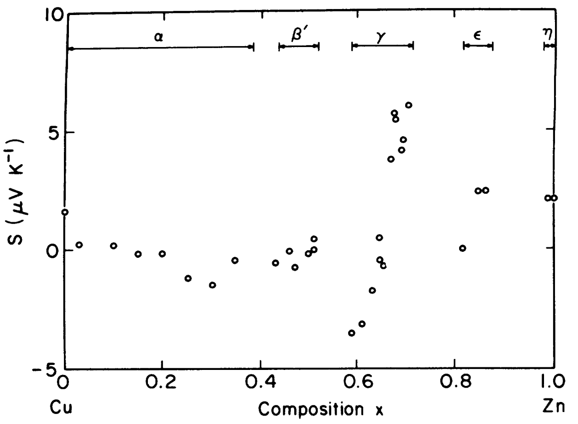

FIG. 9. Variation of thermoelectric power at 295 K as a function of composition $x$ in $Cu_{1-x}Zn_x$ alloys.

*Cu*Al and *Cu*Zn shows an initial decrease for small solute concentrations. This behavior has been observed in many noble metal alloys involving polyvalent solutes.[15] It is interesting that *Al*Cu shows an extremely large change of thermoelectric power upon alloying, in contrast to *Al*Zn and *Al*Mg which have much more extensive ranges of solubility.[16] As expected, the thermoelectric power changes with composition very rapidly in the $\gamma$ phase of both systems. There is a change of sign at approximately 67.5 at. % zinc and 33 at. % aluminum, which values are near those corresponding to the observed minima in resistivity. From Fig. 9, it can be seen that, in the case of $\gamma$-CuZn, there is evidence for a local minimum in the thermopower near the upper stability limit of the phase. This behavior is correlated with the observed composition dependence of resistivity, which has a local maximum in the same range. The present data for both systems are similar to those previously reported,[6] with the exception that the magnitude and sharpness of the discontinuity in $S$ is here more pronounced.

## IV. DISCUSSION

The foregoing experimental results will now be analyzed for electronic effects, after a brief review of the band structure for the various phases of the copper-aluminum and copper-zinc systems.

### A. Band structure

The electronic band structure of the primary solutions *Cu*Al, *Cu*Zn, and *Al*Cu is well understood. Recent de Haas—van Alphen (dHvA) experiments[17] have shown that the Fermi surfaces of dilute *Cu*Al and *Cu*Zn alloys are similar to that of copper, contact occurring across the {111} Brillouin zone (BZ) faces. Alloying increases the so-called belly and neck radii of the Fermi surface, the rate of increase of each dimension with electron concentration being close to those predicted by the rigid-band model. Position annihilation studies[18] give essentially similar results for more concentrated *Cu*Zn and *Cu*Al alloys, in agreement with recent theoretical band calculations.[19] The density of states at the Fermi level decreases with increasing electron/atom ratio, as in the rigid-band model.

The effect of alloying on the *Al*Cu system has also been investigated using the dHvA effect. In this case the results are consistent with an analysis based on the Kohn-Korringa-Rostoker (KKR) or phase-shift method.[20] No experimental dHvA information is available for the *Zn*Cu hexagonal $\eta$ phase. The only model that has been used for the interpretation of electronic specific-heat data for this phase is that due to Hume-Rothery and Jones, which has also been applied to the $\epsilon$ phase.[21]

Of the intermediate phases in both systems, the ordered $\beta'$-CuZn and $\theta$-CuAl$_2$ have been studied in detail using the dHvA effect.[22,23] In the former case, extensive magnetoresistance data as well as band calculations[24,25] have given a very complete picture of its electronic structure. Basically the Fermi surface can be pictured in terms of a simple two-band model, corresponding to a first-zone hole surface and a complex second-zone electron surface in the relevant cubic BZ for this phase. The band structure of CuAl$_2$ can be described, at least in the lowest approximation, by the nearly-free electron model.

The electronic structure of $\gamma$-CuZn, as well as the related $\gamma_2$ and $\theta$ phases of the copper-aluminum system, conforms to the well-known Jones model.[26] This model assumes that the stability of the $\gamma$ phase is correlated with overlap between the Fermi sphere and the {311} and {440} faces of the so-called Jones zone. These faces, which are all equidistant from $\vec{k}=0$, are characterized by the largest nonvanishing structure factor for the $\gamma$-brass unit cell. Contact between the sphere and the faces of the Jones zone occurs at the electron concentration $9\pi/13\sqrt{2}=1.54$ states per atom. Beyond this critical value, the Fermi surface to lowest order consists of a sphere truncated by the zone faces. Correspondingly, the Fermi-surface area and density of states at the Fermi level decrease sharply as a function of electron/atom ratio. Measurements of the electronic specific heat for $\gamma$-CuZn are in agreement with the latter prediction.[21] No theoretical information is available about the band structure of either the $\zeta_2$ or $\eta_2$ phases of the copper-aluminum system.

### B. Resistivity

The initial values of $d\rho/dc$ for the cubic primary solid solutions *Cu*Al, *Cu*Zn, and *Al*Cu are $1.30\pm0.10$, $0.33\pm0.02$, and $0.95\pm0.10$ $\mu\Omega$ cm per atomic percent, respectively. For the first two phases, the ratio of slopes is

$$\frac{\left[\dfrac{d\rho}{dc}\right]_{Cu\text{Al}}}{\left[\dfrac{d\rho}{dc}\right]_{Cu\text{Zn}}}=3.9\pm0.3\ , \tag{1}$$

which is close to the value of 4 predicted by the Nordheim relation.[27] Therefore, the impurity scattering is close to ideal, in that the dominant phase shift in each alloy corresponds to the $l=1$ partial wave. In the case of *Al*Cu, it has been previously demonstrated[7] that the scattering is affected by the different lattice parameters of aluminum relative to copper and the increased importance of the $l=0$ partial wave.

For the hexagonal $\eta$-phase *Zn*Cu the initial slope $d\rho/dc$ is $0.50\pm0.03$ $\mu\Omega$ cm per atom percent, which is considerably larger than that for *Cu*Zn. In order to explain this result it is again necessary to invoke substantial $s$-wave ($l=0$) scattering. No theoretical band calculations have been made for zinc-based alloys, so that it is not possible at present to check this conclusion.

The full curves in Figs. 1 and 2 are the predicted behavior of the two alloy systems according to a generalized virtual-crystal model, considering only effects due to changes in composition and neglecting changes in crystal structure. For the alloy $A_cB_{1-c}$, it is easily shown that the impurity resistivity $\rho$ is given:

$$\rho=c(1-c)[\alpha_1+(\alpha_2-\alpha_1)c]\,|M\,|^2, \tag{2}$$

where $M$ is the matrix element of the difference potential $(V_A-V_B)$ and $\alpha_1,\alpha_2$ take into account the difference of valence between the constituents $A,B$. Here the values of $\alpha_1$ and $\alpha_2$ have been chosen to fit the initial slopes of the primary solid solutions. It is clear that the data for $\gamma$-CuZn, as well as $\gamma_2$- and $\delta$-CuAl, conform better to the predicted behavior than do the other phases. This circumstance simply results from the fact that the former alloys are disordered systems, in contrast to the latter which are ideally stoichiometric electron compounds. In particular, the resistivity of the $\beta'$ phase of copper-zinc deviates more from the curve in Fig. 2 as the composition approaches the equiatomic composition, corresponding to perfect order.

The resistivity of the $\gamma$-phase alloys depends very strongly on composition, a pronounced minimum being observed in both systems. It is believed that this behavior is associated with the electronic structure of this phase. With the usual relaxation time approximation, the conductivity of a cubic metal is given by the equation

$$\sigma=\frac{e^2}{12\pi^3\hbar}\langle \tau v\rangle S_F . \tag{3}$$

In this equation $S_F$ is the Fermi-surface area and $\langle \tau v\rangle$ is the average over the surface of the product of the relaxation time $\tau$ and the carrier velocity $v$. The present data suggest that the increase in resistance beyond the minimum is associated with the rapid decrease in $S_F$ with electron/atom ratio. Since the carrier velocity $v$ is a slowly varying function of energy, the initial decrease in resistance must be ascribed to a minimum in the scattering rate $1/\tau$. The existence of the latter is presumably due to a corresponding minimum in the density of states, resulting from overlap across the faces of the Jones zone. As will be seen shortly, these overlap effects are evident in a number of the properties of $\gamma$-phase alloys reported in this paper. It is of interest that the observed minimum in the resistivity for $\gamma$ phase of the copper-zinc system is much less pronounced than that for the copper-aluminum system. The reason for this difference is not understood in detail, but is probably caused by minor differences in the electronic structure of the $\gamma_2$ and $\gamma$ phases.

### C. Magnetic susceptibility

For a simple binary alloy $A_cB_{1-c}$ the total magnetic susceptibility can be expressed quite generally in the form

$$\chi=c\chi_A+(1-c)\chi_B+\chi_p+\chi_d . \tag{4}$$

In this equation $\chi_A$ and $\chi_B$ are the susceptibilities of the individual constituent ions, so that the first two terms represent the combined core susceptibility. Of the remaining terms $\chi_p$ is the usual Pauli paramagnetic contribution and $\chi_d$ is the Landau diamagnetic susceptibility due to the conduction electrons. Neglecting exchange corrections, the Pauli susceptibility is given by

$$\chi_p=\mu_0^2 N(E_F), \tag{5}$$

where $\mu_0$ is the Bohr magneton and $N(E_F)$ is the electronic density of states at the Fermi level.

The magnetic behavior of the primary solid solutions is readily understood from Eq. (4). In particular the increase in the diamagnetic susceptibility for *Cu*Al and *Cu*Zn is due to changes in $\chi_p$. This term is proportional to $N(E_F)$ and hence decreases with increasing electron/atom ratio. It is believed that the behavior of *Al*Cu and *Zn*Cu can be explained similarly, the value of $d\chi/dc$ being very large in the former case as a result of the changes in the overall core susceptibility.

The most striking feature of Figs. 3 and 4 is a very large peak in diamagnetic susceptibility of the $\gamma$ phase for both copper-aluminum and copper-zinc. Similar peaks have been also found in other noble-metal alloy systems, e.g., copper-cadium and silver-zinc.[11] As noted previously, $N(E_F)$ has a sharp minimum as a function of electron/atom ratio in the $\gamma$ phase, so that the associated change in $\chi_p$ partly accounts for the observed behavior. However, it seems unreasonable to ascribe the entire effect to this source. Rather, it appears that a major contribution to the diamagnetism arises from the Landau term $\chi_d$. This term is expected to be very large when there is significant contact of the Fermi surface with the Jones zone[28] and should decrease rapidly as overlap effects across the zone faces are initiated. Unlike the behavior of the resistivity data, the peak in the diamagnetism of $\gamma$-CuZn is significantly larger than that in $\gamma_2$-CuAl. Presumably, these differences reflect the differences between the $\gamma$ and $\gamma_2$ structures. It is interesting that the properties of the $\delta$ phase in copper-aluminum are very similar to those of the $\gamma_2$ phase, strengthening the hypothesis that they are not distinct.

The magnetic behavior of both the $\beta'$ phase of copper-zinc and $\epsilon$ phase of copper-aluminum is consistent with the assumption that the changes of susceptibility with composition are again due to the Pauli paramagnetic term $\chi_p$. Electronic specific-heat data show that the density of states $N(E_F)$ in the $\beta'$ phase decreases rapidly with increasing Fermi energy.[21] Hence, there is a corresponding decrease in $\chi_p$ and a net increase in the overall diamagnetism with increasing zinc concentration, in agreement with experiment. Similar arguments apply to the $\epsilon$ phase for increasing copper concentration.

Little detailed information is available about the electronic structure for the remaining $\zeta_2$, $\eta_2$, and $\theta$ phases in the copper-aluminum system. In all three cases there is a net paramagnetic contribution arising from the ion-core and Pauli terms. Since the overall susceptibility is diamagnetic, it must be concluded that there is a large Landau term arising from small pockets of holes, analogous to the situation in $\gamma$-phase alloys.

### D. Hall constant

In the relaxation-time approximation, the Hall coefficient for a Fermi surface consisting of a single sheet is[29]

$$R=\frac{12\pi^3}{ecS_F}\frac{\langle \tau^2 v^2/\rho\rangle}{(\langle \tau v\rangle)^2}. \tag{6}$$

The numerator is again an average over the Fermi surface involving the mean curvature defined by

$$\frac{1}{\rho}=\frac{1}{2}\left[\frac{1}{\rho_2}+\frac{1}{\rho_2}\right], \tag{7}$$

where $\rho_1$ and $\rho_2$ are the principal radii of curvature at the point $\vec{k}$. For isotropic relaxation and a spherical Fermi surface, Eq. (6) reduces to the elementary expression

$$R=\frac{1}{nec}, \tag{8}$$

where $n$ is electron density. By analogy, Eq. (6) can generally be written in the same form, with $n$ being replaced by an effective carrier density $n_{\text{eff}}$.

For a complex Fermi surface, Eq. (6) is readily generalized to include a sum corresponding to the various sheets of the surface. The curvature will change sign for a hole sheet giving a positive contribution to the Hall constant. In the simplest two-band model with spherical energy surfaces and constant relaxation times, we recover the familiar form

$$R=\frac{1}{ec}\frac{n_1\mu_1^2-n_2\mu_2^2}{(n_1\mu_1+n_2\mu_2)^2}. \tag{9}$$

Here $n_1,n_2$ are the respective electron and hole densities, while $\mu_1,\mu_2$ are the corresponding carrier mobilities.

The behavior of the Hall coefficients for the primary solid solutions *Cu*Al and *Cu*Zn is readily understood in terms of the generalized form of Eq. (8). In each case the effective carrier density $n_{\text{eff}}$ increases on alloying, leading to a decrease in the magnitude of the Hall coefficient; the sign of $R$ is negative, corresponding to electron conduction. Both sets of data are roughly identical when plotted in terms of electron concentration, showing that in lowest order the band structure conforms to the rigid-band model.

In the case of *Al*Cu, the data are consistent with the two-band model, assuming that electron mobility is larger than the hole mobility. For pure aluminum, Eq. (9) with $n_1=n_2$ then gives a negative overall Hall coefficient, in agreement with experiment. With increasing solute concentration $n_1$ decreases and $n_2$ increases, giving a net decrease in the magnitude of $R$. As explained previously, data for the hexagonal $\eta$ phase of the copper-zinc system are not reliable because of experimental difficulties associated with large grain size in the specimens. However, from Fig. 6 it is clear that the overall value of the Hall coefficient is positive, corresponding to hole conduction. The effect of alloying copper to zinc would be to decrease the electron density and increase the hole density, so that in this case the value of $R$ should increase with increasing copper concentration. This prediction appears to be consistent with the present data, in spite of the experimental uncertainties.

The most salient feature of Figs. 5 and 6 is the composition dependence of the Hall coefficient for the $\gamma$ phases in both systems. Basically, the behavior can be understood in terms of the two-band model discussed above. For $\gamma$-CuZn the initial rapid increase of $R$ is associated with the decreasing number of holes, as result of contact between the Fermi surface and the Jones zone. Once overlap across the faces has been initiated, there is a competing negative contribution to $R$ arising from the electron states produced by the overlap. Therefore, the overall effect is to produce a sharp maximum as a function of electron/atom ratio, the overall sign of $R$ corresponding to the dominant hole carriers in the incompletely filled Jones zone. In the case of the $\gamma_2$ phase of the copper-aluminum system, the observed behavior suggests the existence of two maxima occurring at different values of electron concentration. This situation could easily occur, since overlap occurs across $\{331\}$ as well as $\{440\}$ faces of the Jones zone. The energy gap across these faces in the real structure might well be quite different and hence could produce the observed double maximum. It is to be emphasized that this explanation leaves unanswered why the $\gamma_2$ phase behaves differently from the $\gamma$ phase in this respect.

Little can be said about the behavior of the other intermediate phases in the copper-aluminum system. Clearly the two-band model can be invoked to explain the positive Hall coefficients for the $\zeta_2$ and $\eta_2$ phase and the essentially zero value for the $\theta$ phase. However, there is little additional theoretical justification for this procedure. For $\beta'$-CuZn the concentration dependence of $R$ is most easily understood if the Fermi surface is remapped into the BZ for a bcc structure. The resulting volume and hence effective carrier density is then easily seen to increase with increasing zinc concentration, leading to a reduction in Hall coefficient in accord with experiment. If the energy gaps across the zone faces in both the fcc and bcc structures are ignored, then the variation of $R$ with electron/atom ratio should lie on the same curve for both the $\alpha$ and $\beta'$ phases. As can be seen from Fig. 6, this prediction is approximately correct.

### E. Magnetoresistance

The transverse magnetoresistance for the simple two-band model, discussed in the preceding section, is given by the expression[30]

$$\frac{\Delta\rho}{\rho}=\frac{\sigma_1\sigma_2(\sigma_1/n_1+\sigma_2/n_2)^2(H/ec)^2}{(\sigma_1+\sigma_2)^2+\sigma_1^2\sigma_2^2(n_1^{-1}-n_2^{-1})^2(H/ec)^2}\,. \tag{10}$$

Here $\sigma_1,\sigma_2$ are the respective conductivities for the two bands in zero field and $\Delta\rho$ is the change in resistivity corresponding to the applied field $H$. In the limit that $\sigma_2$ tends to zero, we recover the usual result that there is no magnetoresistance for a single spherical band in the relaxation-time approximation.

For the $\gamma$-brass structure the Jones zone is incomplete, so that in effect $n_2,\sigma_2$ are finite across the entire range of phase stability. If overlap effects are small, then we have

$$\frac{\Delta\rho}{\rho}=\frac{\sigma_1\sigma_2}{n_1^2}\left[\frac{H}{ec}\right]^2, \tag{11}$$

which can be written as

$$\frac{\Delta\rho}{\rho}=\frac{1}{\rho_1\rho_2}\frac{1}{n_1^2}\left[\frac{H}{ec}\right]^2. \tag{12}$$

In this equation $\rho_1$ and $\rho_2$ are the resistivities of the first and second bands, respectively. If the former is dominant in the conduction process, it can be seen from (12) that the magnetoresistance coefficient $A$ should be inversely proportional to the zero-field resistivity. Comparison of Figs. 1 and 2 with Fig. 7 shows that this prediction is approximately obeyed. However, it is to be emphasized that this simple model does not explain the magnitude of $A$ in any satisfactory way.

### F. Thermoelectric power

For a cubic metal, in the relaxation time approximation, the thermoelectric power is given by the expression[31]

$$S=\frac{\pi^2}{3}\frac{k_B^2T}{e}\left[\frac{d\ln\sigma}{dE}\right]_{E=E_F}. \tag{13}$$

The energy-dependent conductivity $\sigma(E)$ is defined analogously to Eq. (3), except that the integral of $\tau v$ is taken over the surface of constant energy corresponding to $E$. Since $d/dE=(d/dn)(dn/dE)$, the above expression can be rewritten in the form

$$S=\frac{\pi^2}{3}\frac{k_B^2T}{|e|}\left[N(E)\frac{d\ln\rho}{dn}\right]_{E=E_F}, \tag{14}$$

where $|e|$ is the absolute value of the electron charge.

In the primary solid solutions $N(E)$ does not change very rapidly, so that Eq. (14) would predict a decrease in thermopower with increasing solute concentration as a result of the term $d(\ln\rho)/dn$. This prediction is in agreement with experiment, although the sharpness of the initial decrease suggests that the observed behavior is at least in part due to an additional contribution to $S$ arising from phonon drag.[31] For aluminum the latter is known to be quite large, leading to the very large effect of alloying which occurs in *Al*Cu.

As can be seen from Figs. 8 and 9, the thermoelectric power of both $\gamma_2$-CuAl and $\gamma$-CuZn depends very sensitively on composition and in fact changes sign. This behavior is readily understood from Eq. (14), which shows that the discontinuous change in slope for the resistivity $\rho$ should give rise to a corresponding discontinuity in $S$. In particular, the latter should abruptly change sign from a negative to positive value. The actual change does in fact conform to this prediction, although it occurs over a range of electron concentration, presumably as a result of microscopic inhomogeneities in the alloys. However, it is clear that the zero in the thermoelectric power does in fact correspond clearly to the observed minimum in $\rho$. From Fig. 9 it can also be seen that there is evidence for a local minimum in $S$ near the upper limit of stability for $\gamma$-CuZn. This minimum appears to correlate with the additional structure in the behavior of resistivity for higher zinc concentrations, lending support to the hypothesis that the effects on $S$ due to changes in the density-of-states and the phonon drag are insignificant.

Little quantitative comment can be made about the other intermediate phases in either system. However, it is of interest that the thermopower of the $\epsilon$-CuZn phase seems also to exhibit a strong concentration dependence. Probably this is also due to an electronic effect.

## V. CONCLUSIONS

Magnetic susceptibility and transport measurements have been made on bulk alloys covering the copper-aluminum and copper-zinc phase diagrams. Anomalous behavior is observed in all the properties of $\gamma$-phase alloys in both systems. The correlation between these anomalies strongly suggests that they are electronic in origin and are associated with overlap between the Fermi surface and the Jones zone for the $\gamma$-brass structure. Electronic effects have also been observed in the properties of other phases in each system.

## ACKNOWLEDGMENTS

Thanks are due to Mr. C. V. Macchioni, who prepared the resistivity samples for the copper-aluminum system and who made the corresponding resistivity measurements. This work was supported by the National Science Foundation under Grant No. DMR-79-23355.

---

[1] C. Macchioni, J. A. Rayne, and C. L. Bauer, Phys. Rev. B 25, 3865 (1982).

[2] See for example, W. B. Pearson, *Handbook of Lattice Spacings and Structures of Metals* (Pergamon, New York, 1958).

[3] J. A. Rayne, M. P. Shearer, and C. L. Bauer, Thin Solid Films 65, 381 (1980).

[4] J. O. Linde, Ph.D. thesis, Lund University, 1939 (unpublished).

[5] A. T. Robinson and J. E. Dorn, J. Metal. Trans. 3, 457 (1951).

[6] Yoshihiro Hishiyama, J. Phys. Soc. Jpn. 22, 449 (1967).

[7] A. Menth, Phys. Kondens. Mater. 6, 145 (1967).

[8] H. Endo, Sci. Rep. Tohoku Imp. Univ. 14, 479 (1925).

[9] W. G. Henry and J. L. Rogers, Philos. Mag. 1, 237 (1956).

[10] Klaus Grube and Ernst Wachtel, Z. Metallkd. 67, 348 (1976).

[11] C. S. Smith, Physics 6, 47 (1935).

[12] W. Köster and H.-P. Rave, Z. Metallkd. 56, 846 (1965).

[13] Kiyoshi Yonemitsu and Sennosuke Takahashi, J. Phys. Soc. Jpn. 27, 352 (1969).

[14] K. Takano, J. Phys. Soc. Jpn. 26, 362 (1969).

[15] R. S. Crisp, W. G. Henry, and P. A. Schroeder, Philos. Mag. 10, 553 (1964).

[16] R. P. Huebner, Phys. Rev. 171, 634 (1968).

[17] P. T. Coleridge and I. M. Templeton, Can. J. Phys. 49, 2449 (1971).

[18] See for example, S. Berko and J. Mader, Phys. Condens. Matter 19, 404 (1975).

[19] A. Bansil, Solid State Commun. 16, 885 (1975).

[20] P. T. Coleridge (private communication).

[21] T. B. Massalski and U. Mizutani, Prog. Mater. Sci. 22, 151 (1978).

[22] J.-P. Jan and C. M. Perrott, J. Low Temp. Phys 8, 195 (1972).

[23] A. E. Dunsworth, J.-P. Jan, and H. L. Skriver, J. Phys. F 9, 1077 (1979).

[24] D. J. Sellmyer, J. Ahn, and J.-P. Jan, Phys. Rev. 161, 619 (1967).

[25] H. L. Skriver and N. E. Christensen, Phys. Rev. B 8, 3778 (1973).

[26] H. Jones, *Theory of Brillouin Zones and Electronic States in Crystals,* (North-Holland, Amsterdam, 1960).

[27] L. Nordheim, Ann. Phys. (Leipzig) 9, 607 (1931); 9, 641 (1931).

[28] H. Jones, Proc. R. Soc. London Ser. A 144, 225 (1934).

[29] M. Tsuji, J. Phys. Soc. Jpn. 13, 979 (1958).

[30] E. H. Sondheimer and A. H. Wilson, Proc. R. Soc. London Ser. A 190, 435 (1947).
London Ser. A 190, 435 (1947).

[31] See, for example, Frank J. Blatt *et al., Thermoelectric Power of Metals* (Plenum, New York, 1976).